Chapter 4

Finite Difference-Collocation Method for Generalized Fractional Diffusion Equation

4.1 Introduction

In this chapter, we study the generalized fractional diffusion equation (GFDE), obtained from the standard diffusion equation by changing the first-order time derivative into a fractional derivative of order $\gamma,\ 0 < \gamma \leq 1$ given as,

$$* \mathcal{D}_{0+}^{\gamma} u(x,t) = \frac{\partial^2 u(x,t)}{\partial x^2} + g(x,t),\ x \in [0,1], \quad t \in [0,\tau], \tag{4.1}$$

with initial and boundary condition,

$$\begin{cases} u(x,0) = \eta_1(x),\ 0 \leq x \leq 1, \\ u(0,t) = \eta_2(t),\ u(1,t) = \eta_3(t), \quad 0 \leq t \leq \tau, \end{cases} \tag{4.2}$$

where $g(x,t)$ is the source/sink function. Whereas, $z(t)$ and $w(t)$ denotes the scale function and weight function respectively. Scale function $z(t)$ effects on the solution to enlarge/contract the solution for increasing and decreasing choices of $z(t)$.

The motive of the chapter is to construct an efficient method to obtain the numerical solution of GFDE. The present method is based on the finite-difference and collocation method. Jacobi polynomials are used as a basis. The outline of the chapter is as follows: In introduction, we discussed some basic facts about FC and Jacobi - polynomials which are needed throughout this chapter. In Section 4.2, first, the finite difference method is used to discretize the time derivative. Second, on the space variable, we use the collocation method for numerical approximation. Further, we estimated the error and convergence analysis analytically, which defines the numerical applicability of the proposed method discussed in Section 4.3. In Section 4.4, we present two numerical examples to validate the proposed method. Also, we compare our results with several other methods which are presented in Section 4.4. At last, in Section 4.5, conclusions are discussed.

4.2 Numerical Scheme and Stability Analysis

4.2.1 Discretization in Time Direction

We split the time interval $[0,\tau]$ into $\mathcal{M}$ equal parts having step size $\Delta t = \frac{\mathcal{T}}{\mathcal{M}}$, $\mathcal{M} \in \mathbb{Z}^+$, and choose the node points as $t_r = r(\Delta t),\ r = 0,1,2,...,\mathcal{M}$, with starting point $t_0 = 0$. Assuming $w(t) > 0,\ \gamma \in (0,1)$ and $z(t)$ is monotonic increasing function on $[0,\mathcal{T}]$, such that $\eta = z(s)$ then $s = z^{-1}(\eta)$. The discretization of

generalized fractional derivative of $u(t)$ at node t_r is given as,

$$\begin{aligned}
{}_*\mathcal{D}^{\gamma}_{0+}u(t_r) &= \frac{[w(t_r)]^{-1}}{\Gamma(1-\gamma)}\sum_{l=1}^{r}\int_{t_{l-1}}^{t_l}\frac{[w(s)u(s)]'}{[z(t_r)-z(s)]^{\gamma}}ds,\\
&= \frac{[w(t_r)]^{-1}}{\Gamma(1-\gamma)}\sum_{l=1}^{r}\int_{z(t_{l-1})}^{z(t_l)}\frac{1}{[z(t_r)-\eta]^{\gamma}}.\frac{d[w(z^{-1}(\eta))u(z^{-1}(\eta))]}{dz^{-1}(\eta)}dz^{-1}(\eta),\\
&= \frac{[w(t_r)]^{-1}}{\Gamma(1-\gamma)}\sum_{l=1}^{r}\frac{w(t_l)u(t_l)-w(t_{l-1})u(t_{l-1})}{z(t_l)-z(t_{l-1})}\int_{z(t_{l-1})}^{z(t_l)}\frac{1}{[z(t_r)-\eta]^{\gamma}}d\eta+\mathcal{R}_r,\\
&= \frac{[w(t_r)]^{-1}}{\Gamma(2-\gamma)}\sum_{l=1}^{r}q_l[w(t_l)u(t_l)-w(t_{l-1})u(t_{l-1})]+\mathcal{R}_r, \qquad (4.3)
\end{aligned}$$

where

$$q_l=\frac{[z(t_r)-z(t_{l-1})]^{1-\gamma}-[z(t_r)-z(t_l)]^{1-\gamma}}{z(t_l)-z(t_{l-1})},\ l=1,2,...r, \qquad (4.4)$$

and $\mathcal{R}_r$ is the truncation error given by

$$\begin{aligned}
\mathcal{R}_r=\frac{[w(t_r)]^{-1}}{\Gamma(1-\gamma)}\sum_{l=1}^{r}\int_{z(t_{l-1})}^{z(t_l)}\frac{1}{[z(t_r)-\eta]^{\gamma}}\Bigg[&\frac{d[w(z^{-1}(\eta))u(x,z^{-1}(\eta))]}{d\eta}-\\
&\frac{w(t_l)u(t_l)-w(t_{l-1})u(t_{l-1})}{z(t_l)-z(t_{l-1})}\Bigg]d\eta.
\end{aligned} \qquad (4.5)$$

Lemma 4.2.1. The coefficient q_l, $l=1,2,...,r$, given in Eq. (4.4), satisfies $q_r > q_{r-1} > ... > q_0 > 0$.

Proof. We shall prove the Lemma 4.2.1 with the help of the mean value property of integrals, $\exists\ f\in[z_{l-1},z_l]$ such that From Eq. (4.4)

$$\frac{q_l}{1-\gamma}=\frac{1}{z_l-z_{l-1}}\int_{z_{l-1}}^{z_l}\frac{1}{(z_r-\eta)^{\gamma}}d\eta, \qquad (4.6)$$

by mean value theorem there exist, $f\in[z_{l-1},z_l]$ such that

$$\frac{q_l}{1-\gamma}=\frac{1}{(z_r-f)^{\gamma}}. \qquad (4.7)$$

4.2.2 Approximation in Space Direction

We apply collocation method to approximate the spatial domain of Eq. (4.1) with Jacobi polynomials. We consider the approximate solution $u_{\mathcal{N}}(x,t)$ of the form as,

$$u_{\mathcal{N}}(x,t) = \sum_{s_1=0}^{\mathcal{N}} c_{s_1}(t)\mathcal{J}_{s_1}^{\alpha,\beta}(x). \tag{4.8}$$

From the Eq. (4.8) and Eq. (4.1), we get

$$* \mathcal{D}_{0+}^{\gamma} u_{\mathcal{N}}(x,t) = \frac{\partial^2 u_{\mathcal{N}}(x,t)}{\partial x^2} + g(x,t), \quad t \in [0,\tau], \tag{4.9}$$

initial and boundary conditions of Eq. (4.1), becomes

$$u_{\mathcal{N}}(x_0,t) = \sum_{s_1=0}^{\mathcal{N}} c_{s_1}(t)\mathcal{J}_{s_1}^{\alpha,\beta}(x_0), \tag{4.10}$$

$$u_{\mathcal{N}}(x_{\mathcal{N}},t) = \sum_{s_1=0}^{\mathcal{N}} c_{s_1} t\mathcal{J}_{s_1}^{\alpha,\beta}(x_{\mathcal{N}}). \tag{4.11}$$

From Eqs. (4.8), (4.3) and Eq. (4.1), we have the semi-discretized scheme as follows

$$\begin{aligned}\sum_{s_1=0}^{\mathcal{N}} \left[\frac{[w(t_r)]^{-1}}{\Gamma(2-\gamma)} \sum_{l=1}^{r} q_l [w(t_l)c_{s_1}(t_l) - w(t_{l-1})c_{s_1}(t_{l-1})] \right] \mathcal{J}_{s_1}^{\alpha,\beta}(x) \\ = \sum_{s_1=0}^{\mathcal{N}} c_{s_1}(t_r) \frac{\Gamma(\alpha+\beta+s_1+3)}{\Gamma(\alpha+\beta+s_1+1)} \mathcal{J}_{s_1-2}^{(\alpha+2,\beta+2)}(x) \\ + g(x,t_r) + \mathcal{R}_r + \mathcal{R}_s, \; r = 1,2,...,\mathcal{M}. \end{aligned} \tag{4.12}$$

where $\mathcal{R}_s$ denote the error term in space direction arise due to replacing $u(x,t)$ with $u_{\mathcal{N}}(x,t)$.

Neglecting the error part we get the fully discretized scheme of Eq. (4.1) by collocation method. We choose the collocation points such that the stability is unchanged.

So we choose the collocation point of the form $x_i,\ i = 1, 2, ...\mathcal{N}-1$, which are the roots of the n^{th} degree Jacobi polynomials and x_0 and $x_{\mathcal{N}}$ are the boundary condition. Thus, for $(x_i, t_r) \in (0,1) \times [0, \tau],\ i = 1, ..., \mathcal{N};\ r = 1, ...\mathcal{M}$, it holds that

$$\begin{aligned}&\sum_{s_1=0}^{\mathcal{N}} \left[\frac{[w(t_r)]^{-1}}{\Gamma(2-\gamma)} \sum_{l=1}^{r} q_l [w(t_l) c_{s_1}(t_l) \mathcal{J}_{s_1}^{\alpha,\beta}(x_i) - w(t_{l-1}) c_{s_1}(t_{l-1}) \mathcal{J}_{s_1}^{\alpha,\beta}(x_i)] \right] \\ &= \sum_{s_1=0}^{\mathcal{N}} c_{s_1}(t_r) \frac{\Gamma(\alpha+\beta+s_1+3)}{\Gamma(\alpha+\beta+s_1+1)} \mathcal{J}_{s_1-2}^{(\alpha+2,\beta+2)}(x_i) + g(x_i, t_r),\ r = 1, 2, ..., \mathcal{M},\end{aligned} \tag{4.13}$$

initial and boundary conditions becomes

$$\begin{cases} u_{\mathcal{N}}(x_i, 0) &= \sum_{s=0}^{\mathcal{N}} c_{s_1}(0) \mathcal{J}_{s_1}^{\alpha,\beta}(x_i) = \eta_1(x_i), \\ u_{\mathcal{N}}(x_0, t_r) &= \sum_{s_1=0}^{\mathcal{N}} c_{s_1}(t_r) \mathcal{J}_{s_1}^{\alpha,\beta}(x_0) = \eta_2(t_r), \\ u_{\mathcal{N}}(x_{\mathcal{N}}, t_r) &= \sum_{s_1=0}^{\mathcal{N}} c_{s_1}(t_r) \mathcal{J}_{s_1}^{\alpha,\beta}(x_{\mathcal{N}}) = \eta_3(t_r). \end{cases} \tag{4.14}$$

In this way, From Eqs. (4.13) - (4.14) we have a system of $(\mathcal{N}+1)$ linear ordinary differential equation in unknown coefficients $c_{s_1},\ s_1 = 0, 1, 2...\mathcal{N}$. We can find the value of unknown coefficients by any standard method. Hence, the approximate solution can be found from the Eq. (4.8).

4.3 Error and Convergence Analysis

In this section, we discuss the error and convergence analysis of the proposed numerical method for Eq. (4.1). We prove the error and convergence analysis analytically with the help of the following lemma and theorems.

Lemma 4.3.1. [129] The truncation error $\mathcal{R}_r$ defined by Eq. (4.5) satisfies,

$$\mathcal{R}_r \leq \left[\frac{1}{8 w_r \Gamma(1-\gamma)} + \frac{\gamma}{2 w_r \Gamma(3-\gamma)} \right] \max_{t_0 \leq \eta \leq t_r} |\mathcal{U}''(\eta)| \mathcal{L} \Delta t^{2-\gamma}, \tag{4.15}$$

where $\mathcal{U}(\eta)$ is the approximating function, w_r is the weight function at node t_r for $r = 1, 2...\mathcal{M}$ and $\mathcal{L}$ is the Lipschitz constant on the interval $[t_{l-1}, t_l]$.

Proof For the detailed proof of this lemma, we refer to [129].

Theorem 4.3.1. The error in approximation of the function $u(x)$ by the first m terms of the series in Eq. (4.8) is bounded by the sum of the absolute values of all the neglected coefficients in the series, i.e.,

$$\mathcal{E}_\tau(\mathcal{N}) = |u(x) - u_{\mathcal{N}}(x)| \leq \sum_{i=m+1}^{\infty} |c_i|, \tag{4.16}$$

$\forall\, u(x), \forall m,$ and $x \in [0, 1]$.

Proof The proof is trivial since $|\mathcal{J}_i^{\alpha,\beta}(x)| \leq 1, \forall x \in [0, 1]$ and $i \geq 0$.

Theorem 4.3.2. Let $u(x, t)$ be the square integrable function defined on $[0, 1]$ and $|u(x, t)| \leq \mathcal{M}_1$, where $\mathcal{M}_1$ is constant. Then the $u(x, t)$ can be expanded with infinite sum of Jacobi polynomials and the infinite series converges to $u(x, t)$ uniformly, i.e.,

$$u(x, t) = \sum_{i=0}^{\infty} c_i(t)\mathcal{J}_n^{\alpha,\beta}(x), \tag{4.17}$$

where

$$|c_i| \leq \frac{\mathcal{M}_2\Gamma(1+\beta)}{\Gamma(2+\alpha+\beta)}\frac{1}{i^3}, \qquad i > 1,$$

$\mathcal{M}_2 = \mathcal{M}_1 \times C$ and $\mathcal{E}_m \to 0$.

Proof From Eqs. (4.8) and (4.9), we have

$$u_m(x, t) = \sum_{i=0}^{m} c_i(t)\mathcal{J}_i^{\alpha,\beta}(x), \tag{4.18}$$

where c_i are the unknown coefficients calculated by

$$\begin{aligned}
c_i(t) &= \frac{1}{\mathcal{H}_i^{\alpha,\beta}} \int_0^1 (x)^\beta (1-x)^\alpha u(x) \mathcal{J}_i^{\alpha,\beta}(x) dx, \\
|c_i| &= \left| \frac{1}{\mathcal{H}_i^{\alpha,\beta}} \frac{1}{t} \int_0^1 (x)^\beta (1-x)^\alpha u(x) \mathcal{J}_i^{\alpha,\beta}(x) \right| dx, \\
&\leq \frac{\mathcal{M}_2}{\mathcal{H}_i^{\alpha,\beta}} \int_0^1 \left| (x)^\beta (1-x)^\alpha \mathcal{J}_i^{\alpha,\beta}(x) \right| dx, \\
&\leq \frac{\mathcal{M}_2}{\mathcal{H}_i^{\alpha,\beta}} \frac{\Gamma(\alpha+i+1)}{i!\Gamma(\alpha+\beta+i+1)} \sum_{m=0}^{i} \binom{i}{m} \frac{\Gamma(\alpha+\beta+i+m+1)}{\Gamma(\alpha+m+1)} \int_0^1 |x^\beta (1-x)^\alpha (x-1)^m| dx, \\
&\leq \frac{\mathcal{M}_2 (2i+1+\alpha+\beta)\Gamma(i+1+\alpha+\beta)\Gamma(1+\beta)}{\Gamma(i+1+\beta)\Gamma(2+\alpha+\beta)} \frac{1}{i^4}, \\
&\leq \frac{\mathcal{M}_2 \Gamma(1+\beta)}{\Gamma(2+\alpha+\beta)} \frac{1}{i^3}.
\end{aligned} \tag{4.19}$$

Hence, the series $u_m(x,t)$ converges to $u(x,t)$ uniformly.

Theorem 4.3.3. Let $h(t)$ be $\mathcal{N}$ times differentiable function defined on interval $[0,\tau]$. Let $u_{\mathcal{N}}(t) = \sum_{j_1}^{\mathcal{N}} c_{j_1} \mathcal{J}_{j_1}^{\alpha,\beta}(t)$ be the approximation of $h(t)$, then

$$\|h(t) - u_{\mathcal{N}}(t)\| \leq \frac{\mathcal{M}\mathcal{S}^{n+1}}{((\mathcal{N}+1)!)} \sqrt{\mathcal{B}_\tau(1+\alpha,\ 1+\beta)}, \tag{4.20}$$

where, $\mathcal{M} = \max_{t\in[0,\tau]} h^{\mathcal{N}+1}(t)$, $\mathcal{S} = \max\{\tau - t_0,\ t_0\}$ and $\mathcal{B}_\tau(1+\alpha,\ 1+\beta)$ denote the incomplete Beta function. At $\tau = 1$, it reduces to the standard Beta function.

Proof By Taylor series expansion, we have

$$h(t) = h(t_0) + h^{'}(t-t_0) + ... + h^{\mathcal{N}}(t_0)\frac{(t-t_0)^{\mathcal{N}}}{\mathcal{N}!} + h^{\mathcal{N}+1}(t)\frac{(t-t_0)^{\mathcal{N}+1}}{(\mathcal{N}+1)!}, \tag{4.21}$$

where $t_0 \in [0, \tau]$ and $\zeta \in [t_0,\ t]$. Let

$$\mathcal{P}_{\mathcal{N}}(t) = f(t_0) + f^{'}(t_0)(t - t_0) + ... + \frac{f^{\mathcal{N}}(t_0)(t - t_0)^{\mathcal{N}}}{\mathcal{N}!}, \tag{4.22}$$

then

$$|h(t) - \mathcal{P}_{\mathcal{N}}(t)| = \left| h^{\mathcal{N}+1}(t) \frac{(t - t_0)^{\mathcal{N}+1}}{(\mathcal{N}+1)!} \right|. \tag{4.23}$$

Since, we assume that $u_{\mathcal{N}}(t)$ is the best square approximation of $h(t)$, we have

$$\begin{aligned}
\|h(t) - u_{\mathcal{N}}(t)\|^2 &\leq \|h(t) - \mathcal{P}_{\mathcal{N}}(t)\|^2, \\
&= \int_0^{\tau} w(t)[h(t) - \mathcal{P}_{\mathcal{N}}(t)]^2 dt, \\
&= \int_0^{\tau} \left[h^{\mathcal{N}+1}(t) \frac{(t - t_0)^{\mathcal{N}+1}}{(\mathcal{N}+1)!} \right]^2 dt, \\
&\leq \frac{\mathcal{M}^2}{((\mathcal{N}+1)!)^2} \int_0^{\tau} (t - t_0)^{2n+2} w(t) dt, \\
&\leq \frac{\mathcal{M}^2 \mathcal{S}^{2n+2}}{((\mathcal{N}+1)!)^2} \int_0^{\tau} (t)^{\beta} (1 - t)^{\alpha} dt, \\
&= \frac{\mathcal{M}^2 \mathcal{S}^{2n+2}}{((\mathcal{N}+1)!)^2} \mathcal{B}_{\tau}(1 + \alpha, 1 + \beta).
\end{aligned} \tag{4.24}$$

Hence,

$$\|h(t) - u_{\mathcal{N}}(t)\| \leq \frac{\mathcal{M}\mathcal{S}^{n+1}}{((\mathcal{N}+1)!)} \sqrt{\mathcal{B}_{\tau}(1 + \alpha,\ 1 + \beta)}. \tag{4.25}$$

Theorem 4.3.4. Let $u(x, t)$ is a continuous function satisfying the conditions (4.2) for any t, and $g(x, t)$ is continuous. Assuming $u_{\mathcal{N}}(x, t_r) = u^r_{\mathcal{N}}(x) = \sum_{s_1=0}^{\mathcal{N}} c_{s_1}(t_r) \mathcal{J}^{\alpha,\beta}_{s_1}(x)$ be the numerical approximation of the scheme (4.13), then the scheme (4.13) is unconditionally stable, and for any $r \geq 0$, it holds that

$$\|u^r_{\mathcal{N}}(x)\|_{L^2} \leq \frac{w_0}{w_r} \|u^0_{\mathcal{N}}(x)\|_{L^2} + \sum_{l=1}^{r-1} \frac{h_l}{w_r} \|g^l\|_{L^2} + \frac{\eta_r}{q_r w_r} \|g^r\|_{L^2}, \tag{4.26}$$

where $g(x,t_r)=g^r(x)$ and $h_l=\left(\frac{1}{q_l}-\frac{1}{q_{l+1}}\right)\eta_l,\ l=1,2,...r-1.$

Proof The proof of this theorem is similar to the Theorem 1 of [129]. In [129], the authors proved the stability for the time-fractional KdV equation. Here, we extend the proof for the time fractional diffusion equation. To prove Theorem 4.3.4, we first rewrite the Eq. (4.12) over the summation up to time step t_{r-1} in discrete form. Thus, we have

$$\frac{1}{\eta_r}q_r w_r u(x,t_r)=\frac{1}{\eta_r}\left[\sum_{l=1}^{r-1}(q_{l+1}-q_l)w_l u(x,t_l)+q_1 w_0 u(x,t_0)\right]+u^{''}(x,t_r)+g(x,t_r), \tag{4.27}$$

where $r=1,2,..\mathcal{M}$ and $\eta_l=w_l\Gamma(2-\gamma)$.

Let $w^{\alpha,\beta}(x)=x^\beta(1-x)^\alpha$ and $u^r_{\mathcal{N}-2}(x)=u_{\mathcal{N}-2}(x,t_r)$ is the a polynomials of $\mathcal{N}-2$ degree satisfying $u^r_{\mathcal{N}}(x)=u^r_{\mathcal{N}-2}(x)w^{\alpha,\beta}(x)$. Multiplying both side in Eq. (4.27) by $u_{\mathcal{N}-2}(x_i,t_r)w^{\alpha,\beta}(x_i)$, and taking summation on i from 0 to $\mathcal{N}$, we have

$$\begin{aligned}\sum_{i=0}^{N}\left[\frac{1}{\eta_r}q_r w_r u(x_i,t_r)\right]u_{\mathcal{N}-2}(x_i,t_r)w^{\alpha,\beta}(x_i)=&\sum_{i=0}^{N}\frac{1}{\eta_r}\left[\sum_{l=1}^{r-1}(q_{l+1}-q_l)w_l u(x_i,t_l)+q_1 w_0 u(x_i,t_0)\right]\\&+\frac{1}{\eta_r}\left[u^{''}(x_i,t_r)+g(x_i,t_r)u_{\mathcal{N}-2}(x_i,t_r)w^{\alpha,\beta}(x_i)\right],\end{aligned} \tag{4.28}$$

where $w^{\alpha,\beta}(x_i)$ is the corresponding weight function. Since degree of $u^r_{\mathcal{N}}$(x) is not exceeding $\mathcal{N}+1$, then from Eq. (2.13),

$$(u^r_{\mathcal{N}},u^r_{\mathcal{N}-2})_{w^{\alpha,\beta}(x)}=(u^r_{\mathcal{N}},u^r_{\mathcal{N}}). \tag{4.29}$$

It can be easily shown that,

$$\int_0^1 u''(x,t_r)u_{\mathcal{N}-2}(x,t_r)w^{\alpha,\beta}(x,t_r)\,dx = \int_0^1 u''(x,t_r)u(x,t_r)w^{\alpha,\beta}(x,t_r)\,dx = 0. \tag{4.30}$$

Now, the discrete form of the Eq. (4.28) at the nodes x_i can be rewritten as

$$q_r w_r \|u^r_{\mathcal{N}}(x)\|_{L^2} \leq \sum_{l=1}^{r-1}(q_{l+1}-q_l)w_l\|u^l_{\mathcal{N}}(x)\|_{L^2} + q_1 w_0 \|u^0_{\mathcal{N}}(x)\|_{L^2} + \eta_r \|g^r(x)\|_{L^2}, \tag{4.31}$$

by using Cauchy-Schwartz inequality and Lemma (4.2.1). The remaining part of the proof can be completed following the similar steps as shown in Theorem 1 of [129].

4.4 Numerical Results

In this section, we provide two numerical examples to validate the presented finite difference-collocation method. In the given examples, we calculate the maximum absolute error (MAE), absolute error (AE), and the order of convergence (CO) for each example. With the help of MAE and CO, we analyze the error and convergence analysis numerically. Also, we have plotted the graphs of the numerical solutions by changing the various parameters like γ, α, β and scale function $z(t)$. For numerical simulations, we take the weight function $w(t) = 1$. All numerical simulations are performed with Mathematica software.

The MAE at time t is given by

$$\mathcal{E}_n(t) = \max_{0\leq x\leq 1} |u(x,t) - u_{\mathcal{N}}(x,t)|, \tag{4.32}$$

and the order of convergence is defined by

$$CO = \frac{log\left(\frac{\mathcal{E}_{n_1}(t)}{\mathcal{E}_{n_2}(t)}\right)}{log\left(\frac{n_2}{n_1}\right)}, \tag{4.33}$$

where $u(x,t)$ and $u_{\mathcal{N}}(x,t)$ are the exact and approximate solutions, respectively. $\mathcal{E}_{n_1}(t)$ and $\mathcal{E}_{n_2}(t)$ are the MAEs for two consecutive values n_1 and n_2.

Example 4.4.1. Here, we consider the generalized version of the problem given in [130] as,

$$* \mathcal{D}_t^{\gamma} u(x,t) - \frac{x^2}{2}\frac{\partial^2 u(x,t)}{\partial x^2} = 0, \quad t \in [0,\tau], \tag{4.34}$$

initial and boundary conditions are given by,

$$\begin{cases} u(x,0) = x^2, \ 0 \leq x \leq 1, \\ u(0,t) = 0, \ u(1,t) = e^{t+\gamma}, \ 0 \leq t \leq \tau. \end{cases} \tag{4.35}$$

The exact solution of Example (4.4.1) is $x^2 e^{t+\gamma}$. This problem is solved for various values of $\mathcal{N}$, $\gamma, z(t)$ and t. In Tables 4.1 and 4.2, we compare the results obtained by our technique to the given methods in [131, 132, 133] at $\gamma = 0$. We observed that the results obtained by the present method (PM) provide a better approximation for this problem. In Table 4.3, we have discussed the MAE and CO for various values of γ and $\mathcal{M}$. Further, In Fig. 4.1, we plot the AEs comparison graphs for different values of γ and observe that the numerical approximation shows good agreement with the exact solution. Fig. 4.2 shows the behavior of the behaviour of the AEs for various values of $\mathcal{N}$ with fix $\gamma = 0.2$. We observe from Fig. 4.2 that the numerical solution at $\mathcal{N} = 6, 8$ shows the good agreement with the exact solution at $\gamma = 0.2$. At last, in Fig. 4.3, we plot the numerical solutions for the various values of $\gamma = 0.1, 0.3, 0.5, 0.7, 0.9$ for a fixed value of $\mathcal{N} = 5$.

TABLE 4.1: Comparison of MAE for Example 4.4.1 with $\gamma = 0.75,\ z(t) = t$.

t	x	Method of [131]	Method of [132]	Method of [133]	Present Method
0.25	0.3	$1.312e-01$	$1.346e-01$	$1.293e-01$	**8.009e-02**
.	0.6	$4.957e-01$	$5.385e-01$	$5.175e-01$	**1.313e-02**
.	0.9	$1.055e-01$	$1.211e-00$	$1.164e-00$	**6.041e-02**
0.5	0.3	$1.685e-01$	$1.795e-01$	$1.695e-01$	**6.342e-02**
.	0.6	$6.303e-01$	$7.183e-01$	$6.780e-01$	**9.543e-02**
.	0.9	$1.352e-00$	$1.616e-01$	$1.525e-01$	**5.315e-02**
0.75	0.3	$2.118e-01$	$2.313e-01$	$2.154e-01$	**5.242e-02**
.	0.6	$7.962e-01$	$9.255e-01$	$8.618e-01$	**6.875e-02**
.	0.9	$1.733e-00$	$2.082e-00$	$1.939e-00$	**4.891e-02**
1	0.3	$2.645e-01$	$2.909e-01$	$2.687e-01$	**4.349e-02**
.	0.6	$9.745e-01$	$1.163e-00$	$1.075e-00$	**4.802e-02**
.	0.9	$2.014e-00$	$2.618e-00$	$2.419e-00$	**1.048e-02**

TABLE 4.2: Comparison of MAE for Example 4.4.1 with $\gamma = 0.9,\ z(t) = t$.

t	x	Method of [131]	Method of [132]	Method of [133]	Present Method
0.25	0.3	$1.122e-01$	$1.218e-01$	$1.210e-01$	**9.795e-02**
.	0.6	$4.762e-01$	$4.872e-01$	$4.841e-01$	**1.543e-01**
.	0.9	$1.046e-00$	$1.096e-00$	$1.089e-00$	**5.303e-03**
0.5	0.3	$1.564e-01$	$1.588e-01$	$1.567e-01$	**7.852e-02**
.	0.6	$6.086e-01$	$6.355e-01$	$6.268e-01$	**1.129e-01**
.	0.9	$1.342e-00$	$1.429e-00$	$1.410e-00$	**9.122e-02**
0.75	0.3	$1.9948e-01$	$2.041e-01$	$1.998e-01$	**6.677e-02**
.	0.6	$7.761e-01$	$8.165e-01$	$7.992e-01$	**9.517e-02**
.	0.9	$1.722e-00$	$1.837e-00$	$1.798e-00$	**5.475e-02**
1	0.3	$2.529e-01$	$2.588e-01$	$2.517e-01$	**5.719e-02**
.	0.6	$9.938e-01$	$1.035e-00$	$1.007e-00$	**6.471e-02**
.	0.9	$2.144e-00$	$2.329e-00$	$2.265e-00$	**1.964e-02**

TABLE 4.3: CO and MAE for Example 4.4.1 with various values of γ and $z(t) = t^2$.

$\gamma = 0.3$			$\gamma = 0.5$		$\gamma = 0.7$	
$\mathcal{M}$	MAE	CO	MAE of PM	CO	MAE of PM	CO
50	$2.637e-01$	...	$4.921e-01$	...	$7.994e-01$	...
100	$9.246e-02$	1.617	$1.839e-01$	1.419	$3.310e-01$	1.263
200	$2.919e-02$	1.663	$6.782e-02$	1.439	$1.380e-01$	1.270
400	$9.186e-03$	1.667	$2.464e-02$	1.460	$5.677e-02$	1.282
800	$2.850e-03$	1.688	$8.878e-03$	1.473	$2.344e-02$	1.275

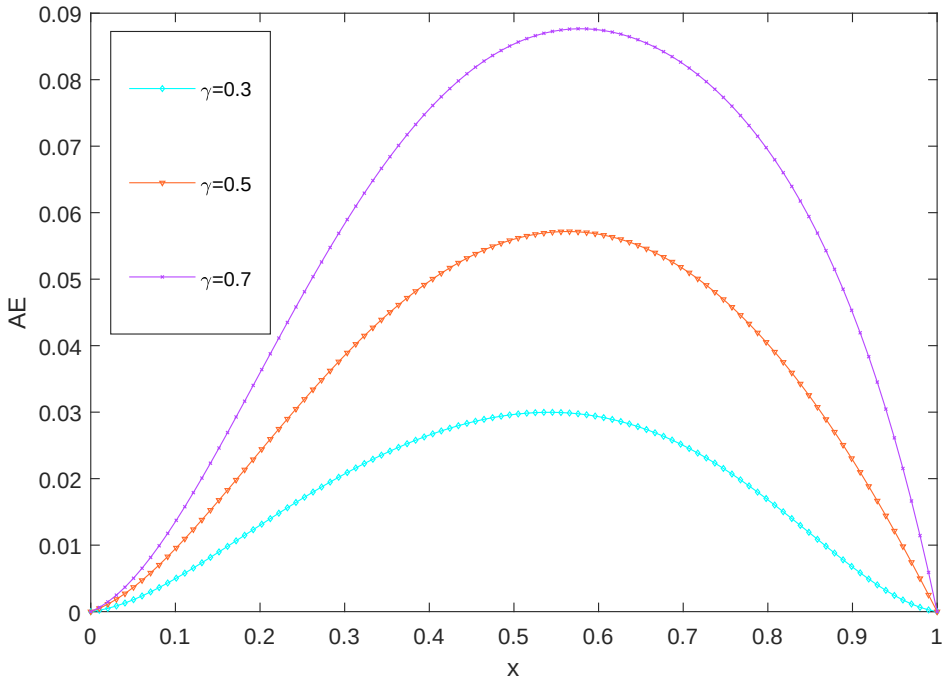

FIGURE 4.1: Comparison of AE at $t = 0.5$, $\mathcal{N} = 5$, $z(t) = t$ and different values of γ for Example 4.4.1.

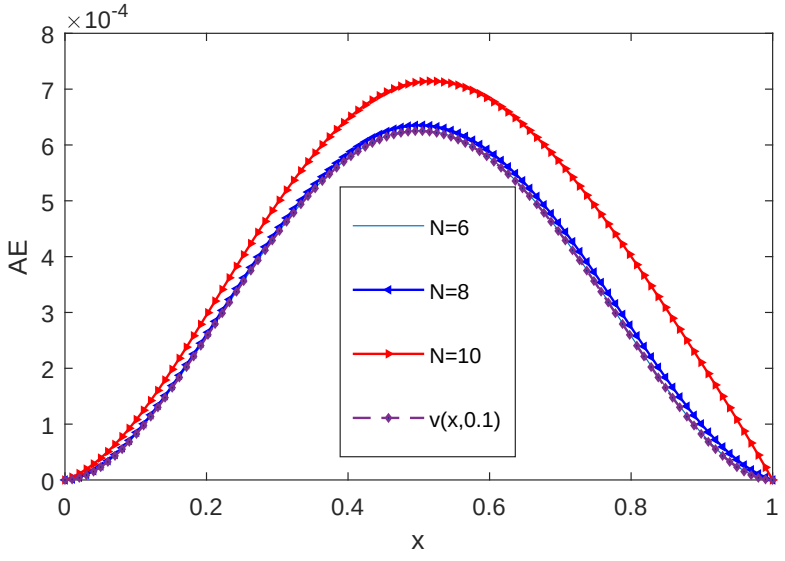

FIGURE 4.2: Plot of AE for different values of $\mathcal{N}$ at $t = 0.1$ and $z(t) = t$ for Example 4.4.1.

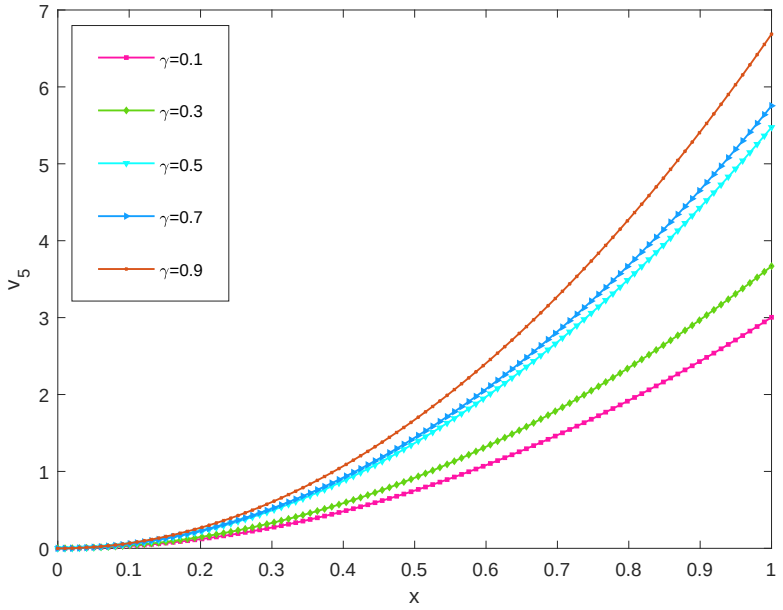

FIGURE 4.3: Comparison of the numerical solution for different values of γ at $t = 1$ and $z(t) = t^2$ for Example 4.4.1.

Example 4.4.2. Consider the following Example [130],

$$* \mathcal{D}_t^{\gamma} u(x,t) = \frac{\partial^2 u(x,t)}{\partial x^2} + g(x,t), \quad t \in [0,\tau], \tag{4.36}$$

where

$$g(x,t) = 4\pi^2 t^2 \sin(2\pi x) + \frac{2t^{2-\gamma}\sin(2\pi x)}{(2-3\gamma+\gamma^2)\Gamma(1-\gamma)},$$

with initial and boundary conditions are given by,

$$\begin{cases} u(x,0) = 0, \\ u(0,t) = 0, \ u(1,t) = 0. \end{cases} \tag{4.37}$$

The exact solution for this Example (4.4.2) is $t^2 \sin(2\pi x)$. We shall apply the numerical scheme (4.12) to solve this problem (4.4.2) for different values of $\mathcal{N}$ with

$z(t) = t$ varying the fractional order $\gamma = 0.1, 0.3, 0.5, 0.7$. We obtain the AEs at the grid points in the given domain which are shown through Tables 4.4 and 4.5, respectively. Results presented through Tables 4.4-4.5 establish the convergence of the proposed method for different values of γ. In Table 4.6, we have shown the MAE by varying the different values of $\gamma = 0.3, 0.5, 0.7$ and $\mathcal{M}$. Further, we show the CO for each value of γ which proves the accuracy of the present method. In Fig. 4.4, we have compared the numerical solutions for various choices of γ with the exact solution known at $\gamma = 0.2$. In Fig. 4.5, the solution graphs for different values of $\mathcal{N}$ and plot of the exact solution(for $\gamma = 0.2$) are shown. From Figs. 4.4 and 4.5, we conclude that the numerical solution obtained by proposed method converges to the exact solution. At last, we compare our results with the existing method [130] in Table 4.7. We see that the proposed method gives better accuracy in approximating the numerical solutions.

TABLE 4.4: Comparison of AE for Example 4.4.2 at $\gamma = 0.1, 0.3$ and various values of $\mathcal{N}$.

	$\gamma = 0.1$			$\gamma = 0.3$		
x	$\mathcal{N} = 5$	$\mathcal{N} = 7$	$\mathcal{N} = 9$	$\mathcal{N} = 5$	$\mathcal{N} = 7$	$\mathcal{N} = 9$
0.1	$5.899e-04$	$4.786e-05$	$2.407e-06$	$5.801e-04$	$4.707e-05$	$2.352e-06$
0.2	$3.927e-04$	$3.174e-05$	$1.694e-06$	$3.801e-04$	$3.074e-05$	$1.618e-04$
0.3	$2.403e-04$	$2.173e-05$	$1.126e-06$	$2.296e-04$	$2.087e-05$	$1.058e-06$
0.4	$1.376e-04$	$1.057e-05$	$5.571e-06$	$1.315e-04$	$1.008e-05$	$5.174e-07$
0.5	$1.051e-18$	$7.952e-20$	$3.281e-19$	$1.233e-04$	$1.067e-18$	$5.225e-19$
0.6	$1.436e-04$	$1.045e-05$	$5.560e-07$	$1.246e-04$	$1.000e-05$	$5.186e-07$
0.7	$2.313e-04$	$2.343e-05$	$1.344e-06$	$2.378e-04$	$2.066e-04$	$1.077e-06$
0.8	$3.567e-04$	$3.164e-05$	$1.678e-06$	$3.875e-04$	$3.099e-05$	$1.623e-06$
0.9	$5.679e-04$	$4.567e-05$	$2.457e-06$	$5.112e-04$	$4.888e-05$	$2.399e-06$

TABLE 4.5: Comparison of AE for Example 4.4.2 at $\gamma = 0.5, 0.7$ and various values of $\mathcal{N}$.

	$\gamma = 0.5$			$\gamma = 0.7$		
x	$\mathcal{N} = 5$	$\mathcal{N} = 7$	$\mathcal{N} = 9$	$\mathcal{N} = 5$	$\mathcal{N} = 7$	$\mathcal{N} = 9$
0.1	$3.386e-05$	$4.579e-05$	$2.194e-06$	$5.350e-04$	$4.407e-05$	$2.406e-06$
0.2	$6.886e-04$	$2.914e-05$	$1.387e-06$	$3.230e-04$	$2.717e-05$	$1.694e-06$
0.3	$8.617e-04$	$1.953e-05$	$8.399e-07$	$1.815e-04$	$1.800e-05$	$1.126e-06$
0.4	$5.455e-04$	$9.335e-06$	$3.863e-07$	$1.047e-04$	$8.528e-06$	$5.570e-07$
0.5	$1.191e-18$	$1.087e-18$	$5.186e-18$	$6.447e-19$	$3.683e-18$	$3.280e-19$
0.6	$5.575e-04$	$9.435e-06$	$3.789e-07$	$1.046e-04$	$8.546e-06$	$5.580e-07$
0.7	$8.637e-04$	$1.944e-06$	$8.457e-07$	$1.824e-04$	$1.890e-05$	$1.136e-06$
0.8	$6.745e-04$	$2.879e-05$	$1.478e-06$	$3.320e-04$	$2.654e-05$	$1.794e-06$
0.9	$3.378e-04$	$4.543e-05$	$2.148e-06$	$5.458e-04$	$4.568e-05$	$2.451e-06$

TABLE 4.6: MAE and CO for Example 4.4.2 for various values of γ and $\mathcal{M}$.

	$\gamma = 0.3$		$\gamma = 0.5$		$\gamma = 0.7$	
$\mathcal{M}$	MAE	CO	MAE of PM	CO	MAE of PM	CO
50	$1.475e-06$	...	$1.718e-06$	...	$3.746e-06$	...
100	$4.636e-06$	1.667	$6.336e-06$	1.439	$1.553e-06$	1.271
200	$1.425e-06$	1.701	$2.300e-06$	1.461	$6.385e-07$	1.282
400	$4.459e-07$	1.676	$8.228e-07$	1.483	$2.613e-07$	1.289
800	$1.387e-07$	1.685	$2.938e-07$	1.485	$1.065e-07$	1.296

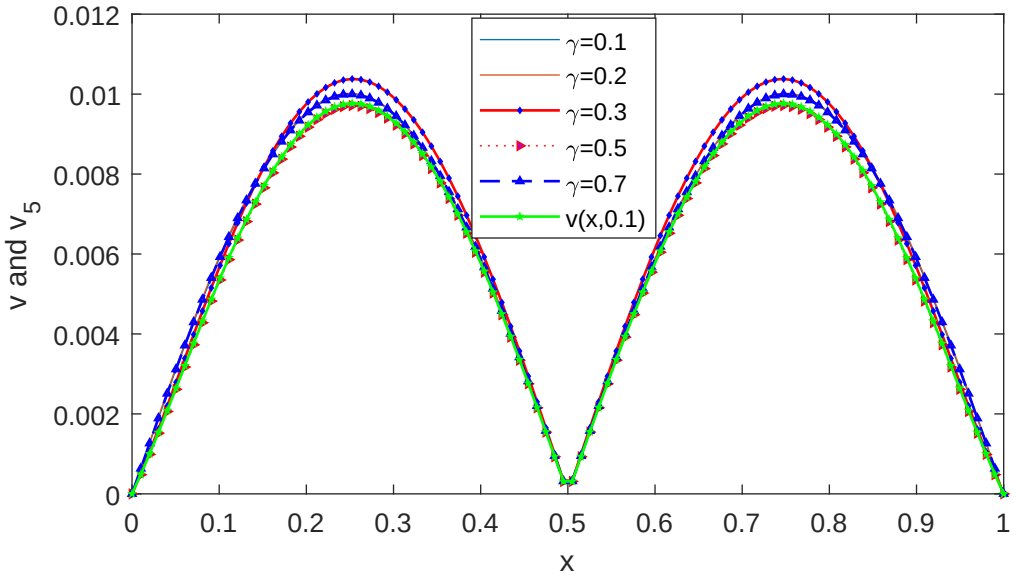

FIGURE 4.4: Comparison of the numerical and the exact solution at $t = 0.1$ and different values of γ for Example 4.4.2.

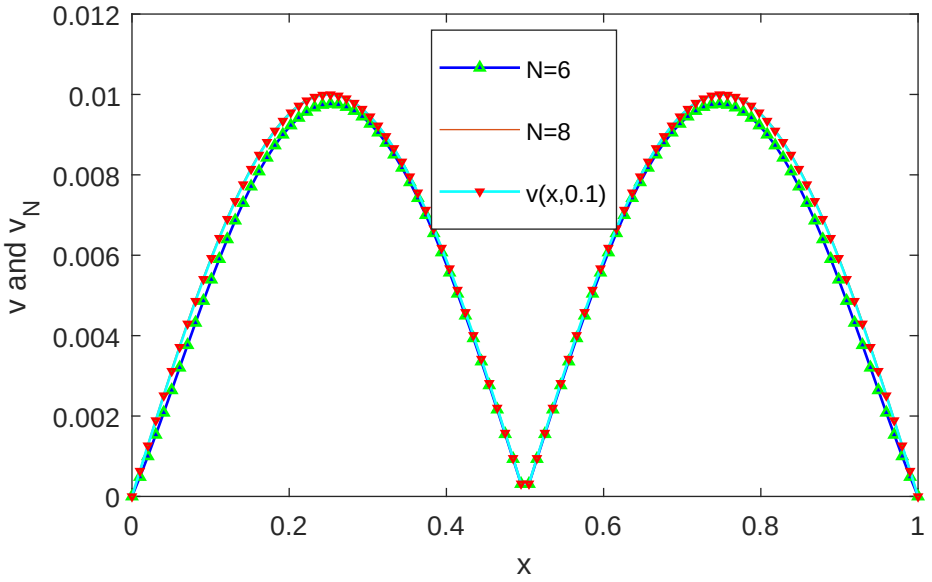

FIGURE 4.5: Plot of the numerical solutions for different values of $\mathcal{N}$ at $t = 0.1$ for Example 4.4.2.

TABLE 4.7: Comparison of MAE of the Example 4.4.2 with $\gamma = 0.5$.

$\mathcal{M}$	Present Method	Method [130]
2	$1.061e-04$	$1.627e-01$
4	$3.879e-05$	$3.101e-02$
6	$2.103e-05$	$1.140e-02$
8	$1.342e-05$	$5.378e-03$
10	$3.925e-06$	$2.726e-03$
12	$7.953e-07$	$1.461e-03$
14	$1.047e-06$	$8.187e-04$
16	$1.252e-06$	$4.755e-04$

4.5 Conclusion

A numerical scheme for a new class of fractional diffusion equation is studied in this chapter in which the time derivative is considered as the generalized fractional derivative. The scheme uses the finite difference and collocation methods to find the numerical solution. The theoretical error and convergence analysis are also validated numerically. Numerical examples show that the proposed method achieves high accuracy in comparison to other methods [130, 132, 133, 134] presented recently.

****